

Programs centered in Dept. 1814 at SNL which fund Microscale Materials Model Development

i) Predicting Performance Margins (PPM):

Connecting nano- and microscale variability to uncertainty in structural metals

Task 1: Nanoscale framework for crack initiation and growth in Ta and Ta alloys.

Task 2: Microscale effects of defect fields in Ta and Ta alloys.

Task 3: Connecting microstructural variability to performance margins in structural metals.

ii) Advanced Certification Program (ACP)

Capturing the physics of the high rate deformation of Ta

Focus: - BCC crystal plasticity constitutive model development

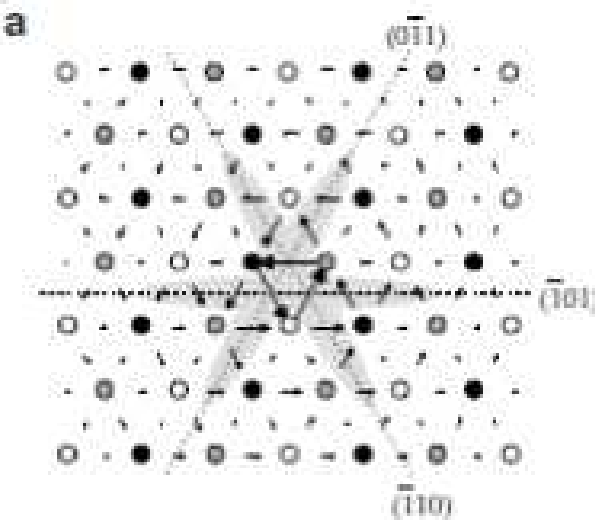
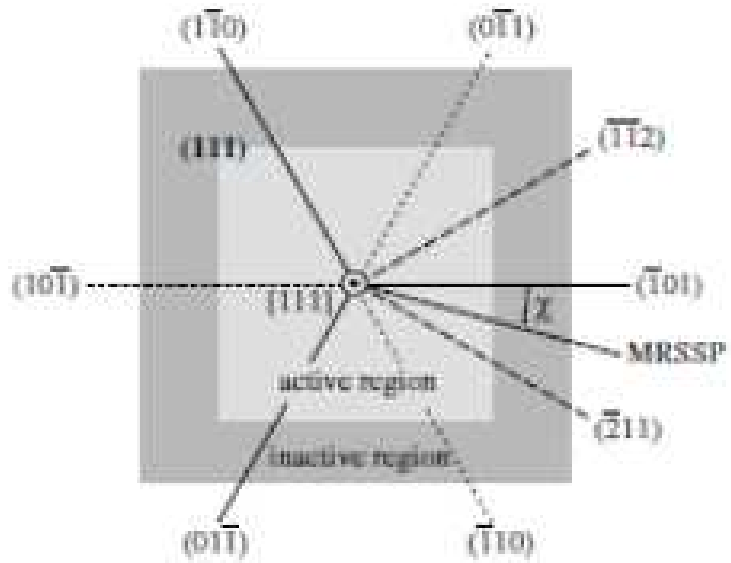
- Incorporating a length scale in polycrystal plasticity models
- Development of 'scale relevant' validation methods.

Primary Collaborators: Corbett Battaile, Chris Weinberger, Liz Holm, Brad Boyce, Blythe Clark

DAGG samples: Eric Taleff and Nick Pedrazas, Univ. Texas

Summary of Atomic Scale simulations for screw dislocation motion in BCC metals

Illustration of Model Geometry



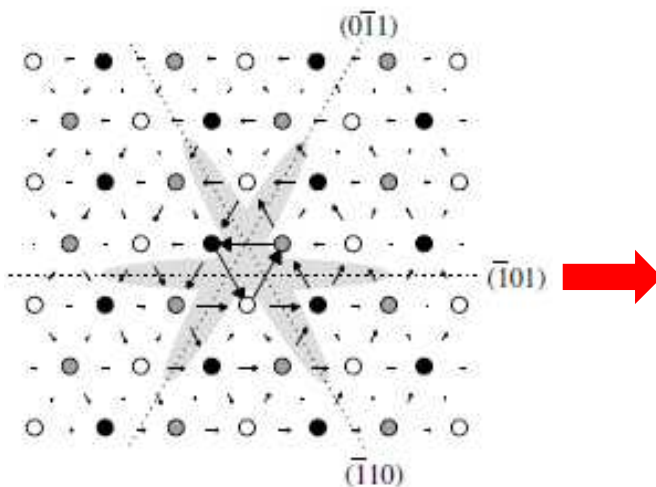
1570 atoms in active region

- Bond order potential model, using potentials for Molybdenum and Tungsten
- Periodic boundary conditions in z-[111] direction (3 planes)
- Insert infinite screw dislocation, allow model to relax

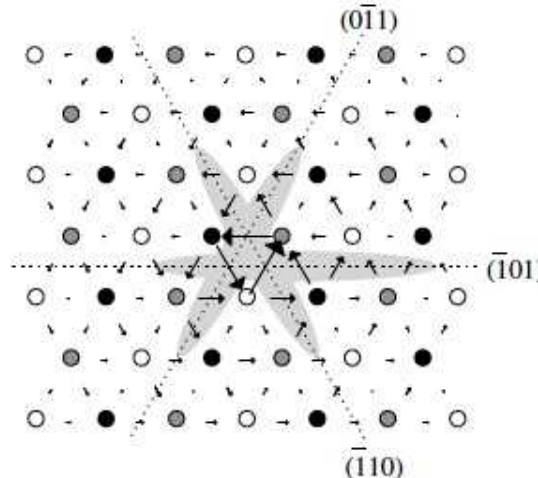
Physical model for dislocation motion in BCC metals

- Simulations reveal the screw dislocation core spreading onto adjacent (110) planes in BCC metals.
 - Core spreading creates a significant Peierls barrier to dislocation motion.
 - Because the dislocation spreads onto three planes, motion can be affected by stress components outside the preferred slip plane, i.e. non-Schmid stresses.

[111] zone depiction of a relaxed screw dislocation core in Mo



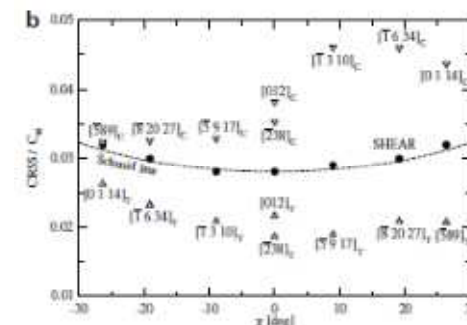
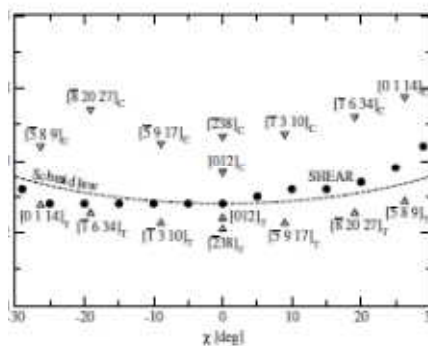
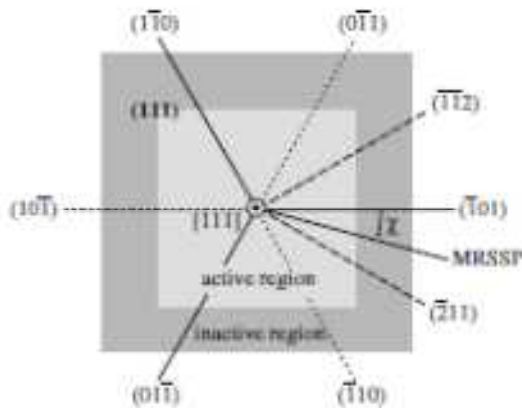
Distortion of the dislocation core under an applied shear stress



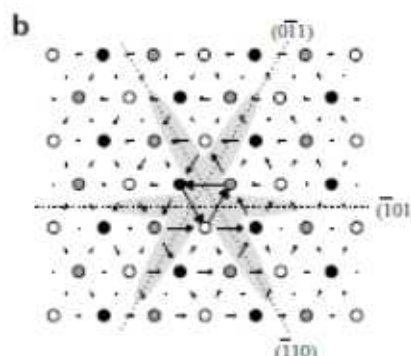
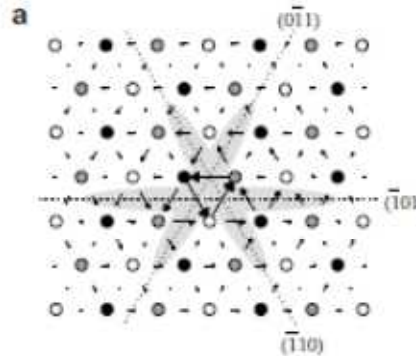
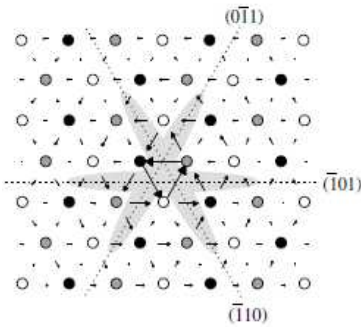
Groger, Vitek et al. *Acta Mat.* **56** (2008) 5412

Simulation studies used to isolate the stresses that initiate dislocation motion

- Load by pure shear in the maximum resolved shear stress plane $\chi < 0$, nearest (112) plane is sheared in the twinning sense, for $\chi > 0$, nearest (112) plane is sheared in the antitwinning sense.
- Loading in Tension and Compression



- Loading by shear stress perpendicular to the slip direction



Yield criterion defined by results from combined shear stress loading in atomistic simulations

Groger and Vitek defined their results in this form:

$$\sigma_{cr}^{app} \left[a_0 \mathbf{m}^{(s)} \mathbf{n}^{(s)} + a_1 \mathbf{m}^{(s)} \mathbf{n}^{(s')} + a_2 (\mathbf{n}^{(s)} \times \mathbf{m}^{(s)}) \mathbf{n}^{(s)} + a_3 (\mathbf{n}^{(s)} \times \mathbf{m}^{(s)}) \mathbf{n}^{(s')} \right] = \tau_{cr}$$

↓ applied stress
 ↓ stress projection tensor, $\mathbf{P}_{\sigma}^{(s)}$
 ↓ yield stress

Parameter	FCC	W	Mo	
a_0	1	1	1	Schmid stress
a_1	0	0	0.24	twinning/anti-twinning
a_2	0	0.56	0	out-of-plane effects
a_3	0	0.75	0.35	out-of-plane effects
τ_{cr}	1	1.36	1.26	

Gap: To develop similar models for other BCC metals, such as Ta and Fe, we need valid interatomic potential functions.

Decomposing resistance to slip in a crystal plasticity model

$$\tau^{(s)} = \mathbf{P}_\sigma^{(s)} : \boldsymbol{\sigma}^{app}$$

$$\dot{\gamma}^{(s)} = \frac{\tau^{(s)}}{\tau_{cr}} \left| \frac{\tau^{(s)}}{\tau_{cr}} \right|^{\frac{1}{m}-1}$$

Plastic strain rate:

$$\mathbf{D} = \sum_s \dot{\gamma}^{(s)} \mathbf{m}^{(s)} \quad \dot{\gamma}^{(s)} = G \left(\frac{\mathbf{m}^{(s)} : \boldsymbol{\sigma}}{\tau^{(s)}} \right)$$

Slip system
FCC: $<110>\{111\}$
BCC: $<111>\{110\}$
m is the same!

$\tau^{(s)}$ is the lattice resistance
on a slip system

$$\tau^{(s)} = \tau(T, \sigma)$$

Decompose τ :

$$\tau(T, \sigma) = \tau_{obs} + \tau_{fric}(T, \sigma)$$

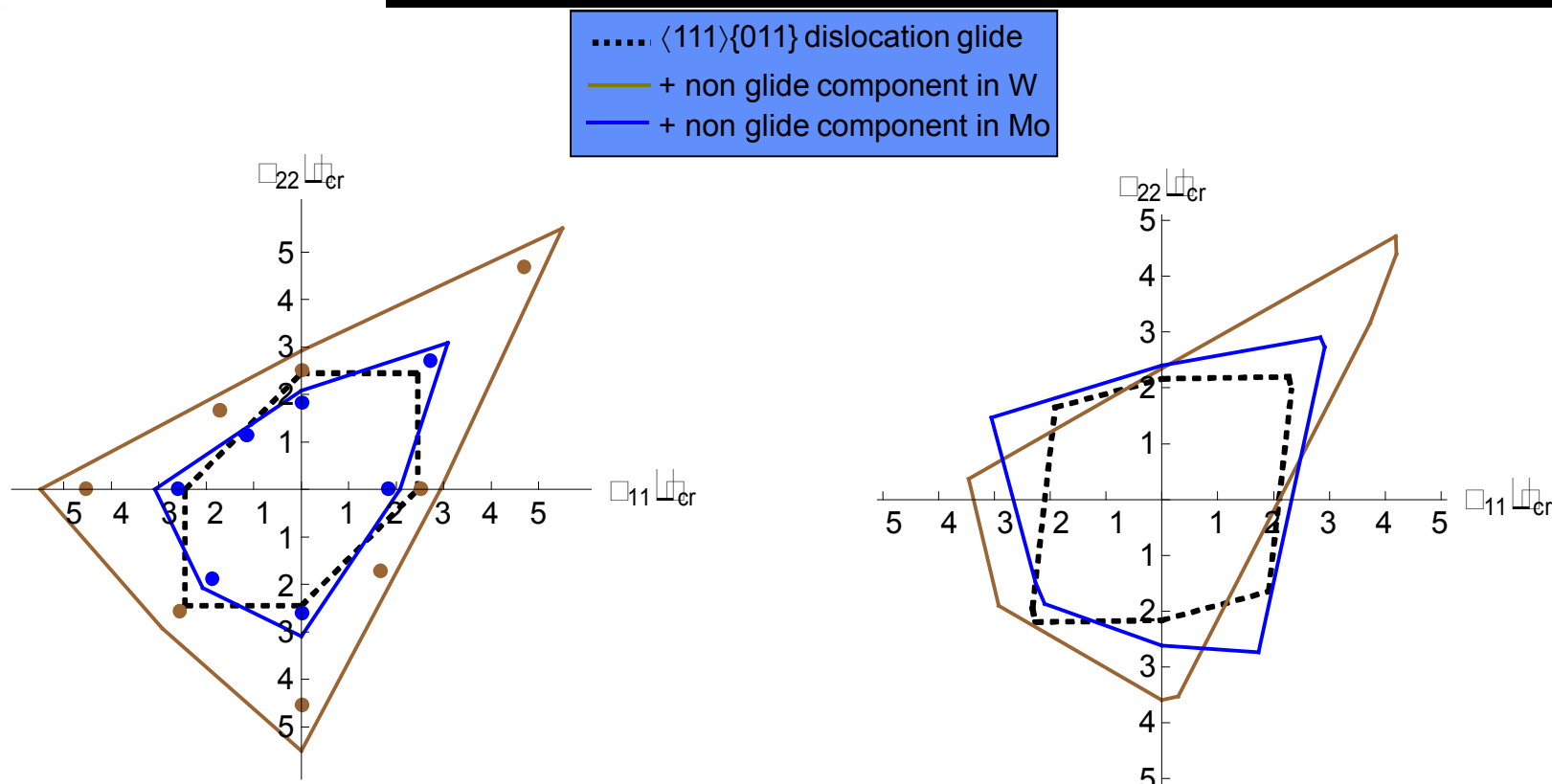
Resistance due to
obstacles, forest
dislocations, etc.
May have T dependence

FCC: $\tau_{obs} \gg \tau_{fric}$ $\tau_{fric} \approx 0$

In BCC metals, screw dislocations have high lattice resistances at low temperatures and control plastic deformation

BCC: $\tau_{fric} \gg \tau_{obs}$

The effect of 'non-schmid' stresses on yield surfaces of BCC single crystals



orientation $-\langle 100 \rangle (010)$
'highly symmetric'

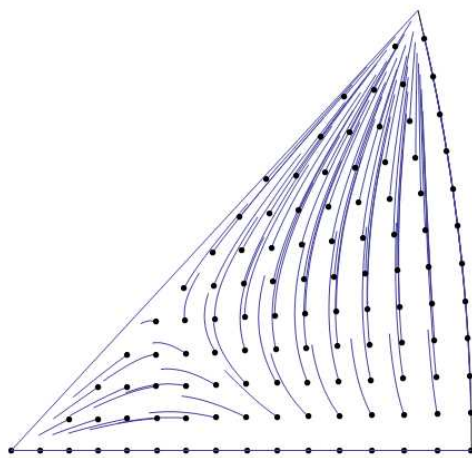
FE implementation- single element

- Tungsten
- Molybdenum

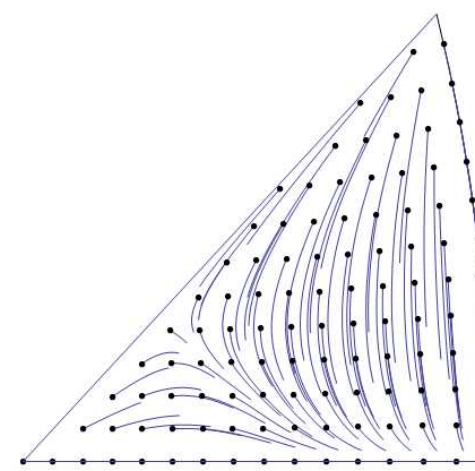
orientation- $\langle -0.180, 0.575, 0.798 \rangle, \langle 0, -0.811, 0.585 \rangle$
'not symmetric'



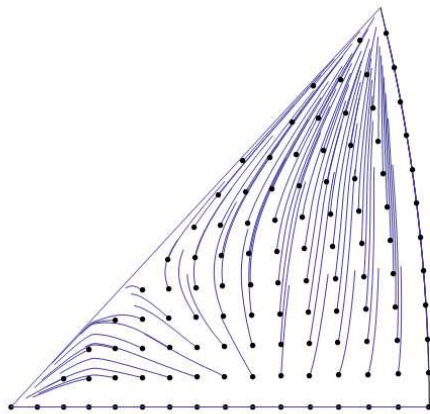
Single Crystal Rotation Paths: Isochoric Deformation to 50% strain



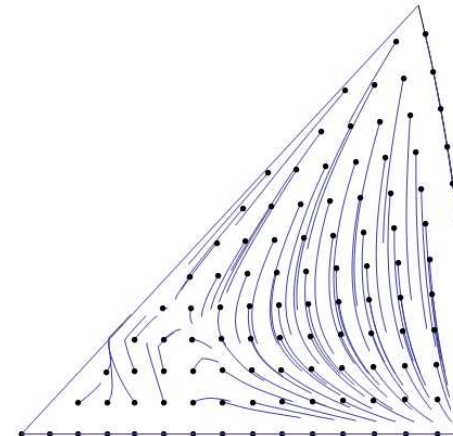
Baseline Compression



Baseline Tension



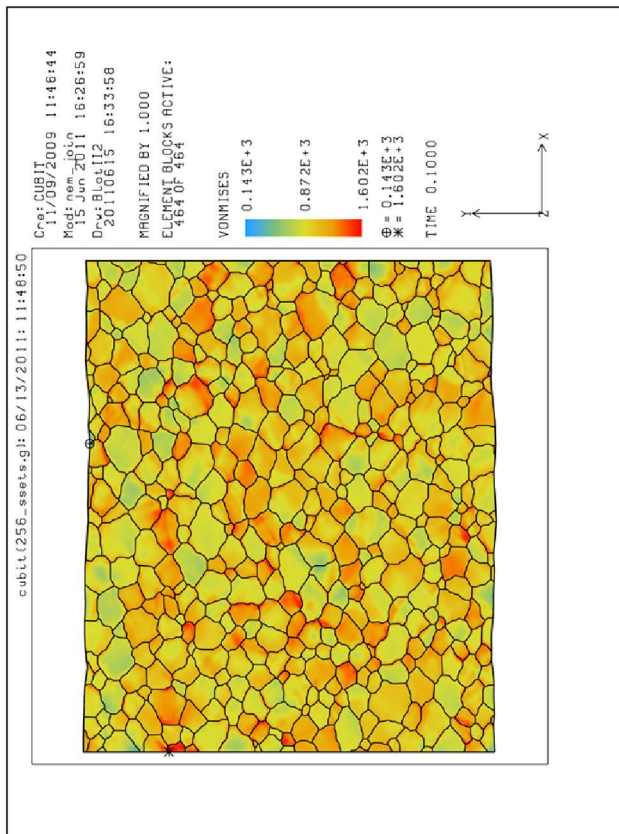
Molybdenum Compression



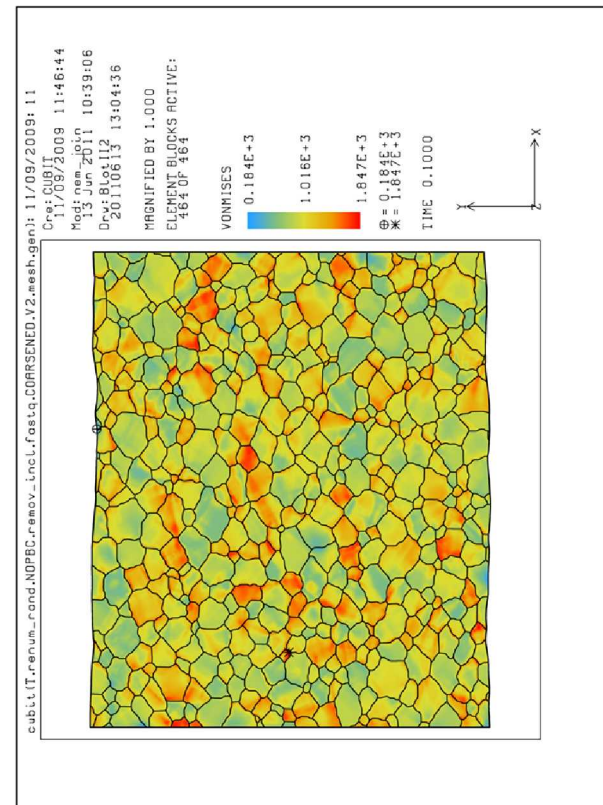
Molybdenum Tension

A comparison of polycrystalline simulations

Tension 10% Strain

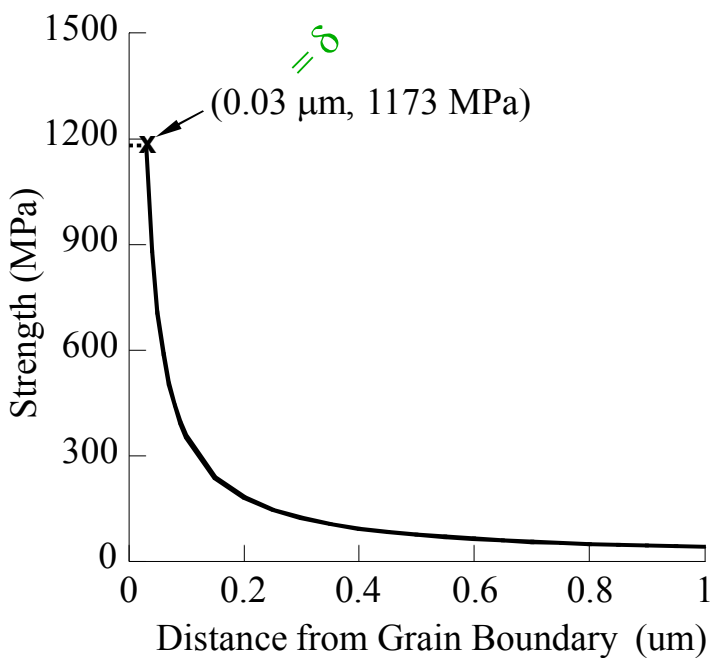


Baseline

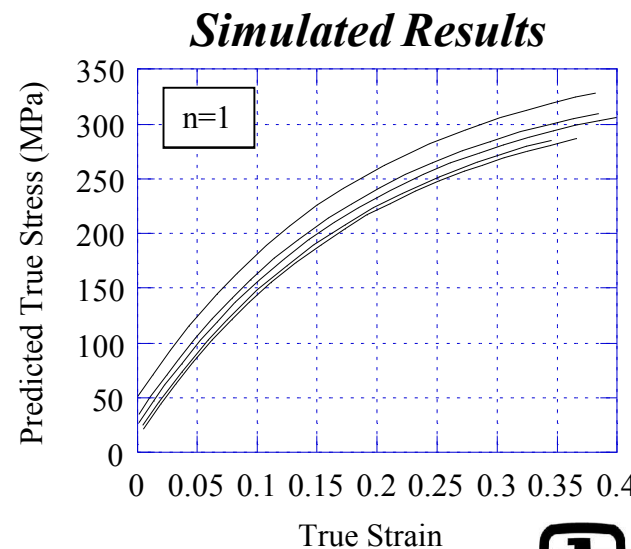
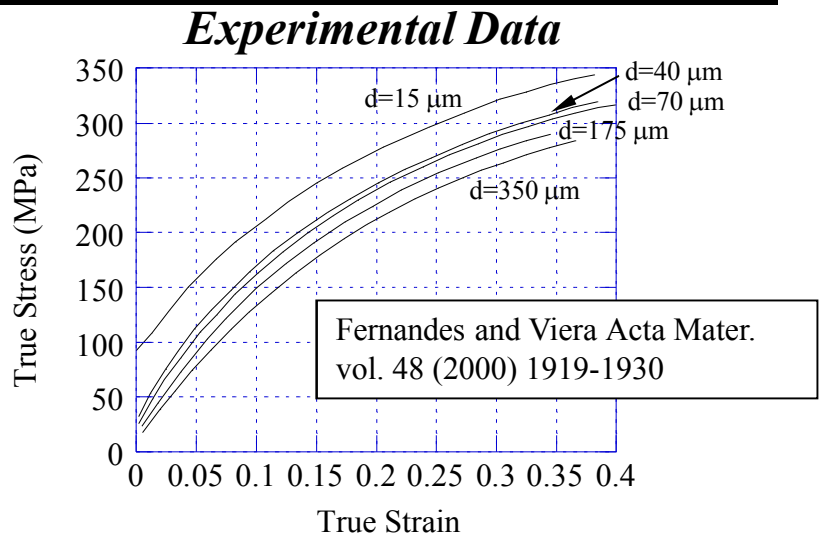


Molybdenum

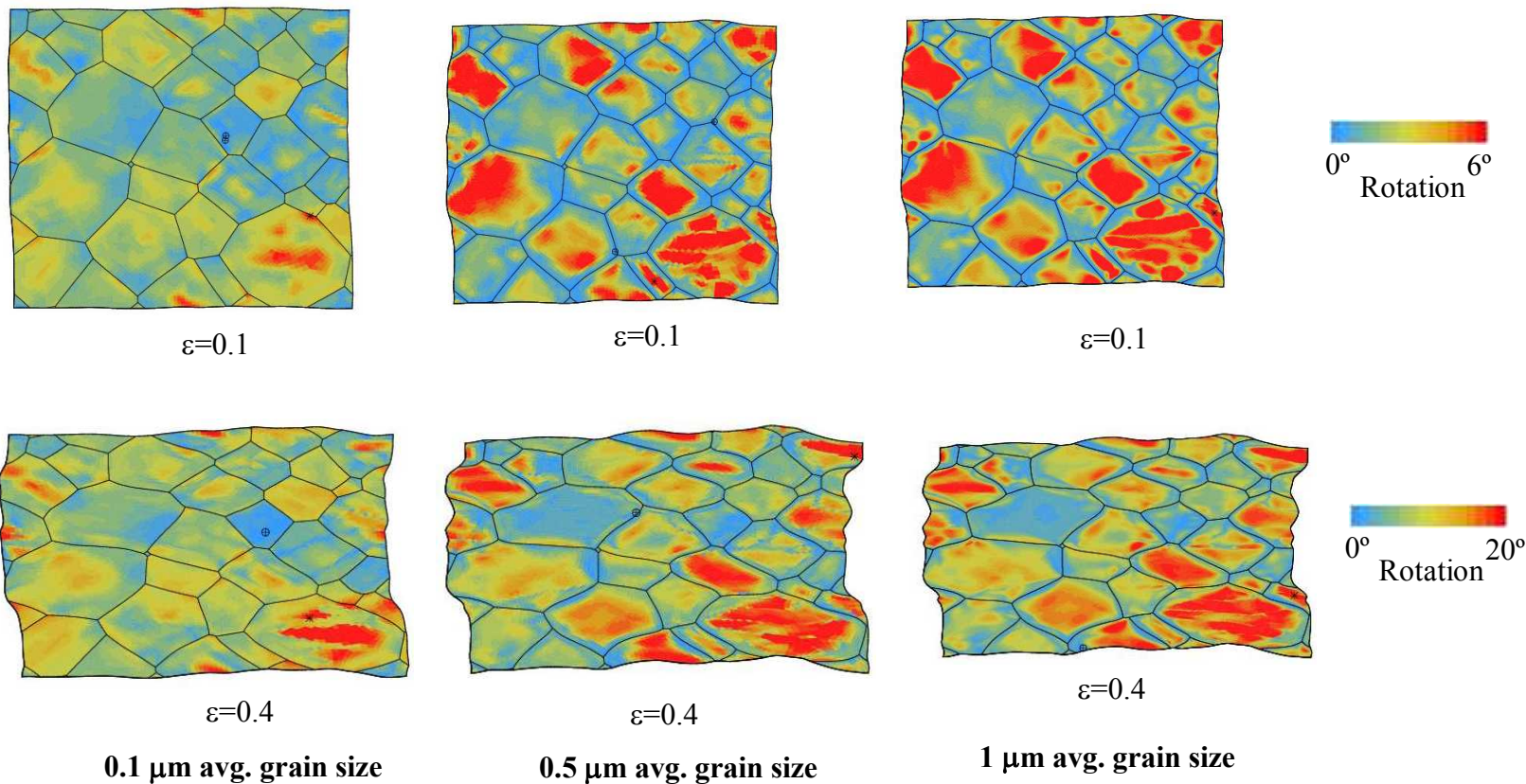
A simple method for incorporating a grain-size driven length scale into a polycrystal plasticity model



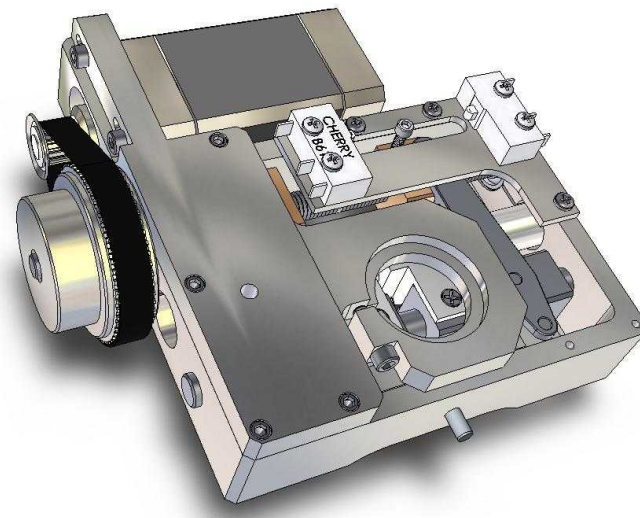
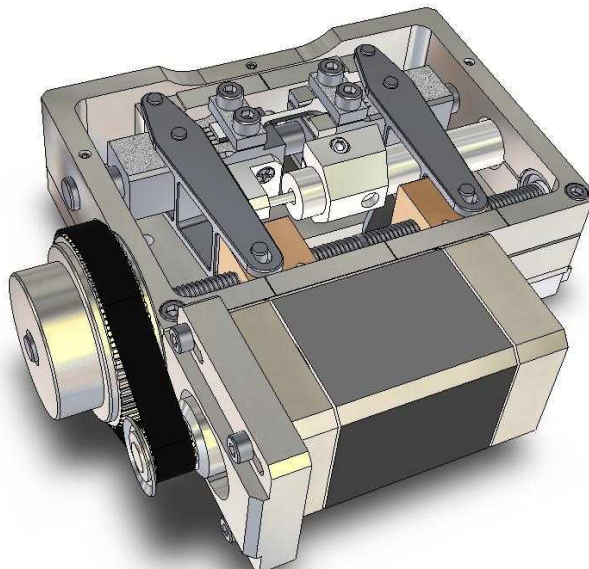
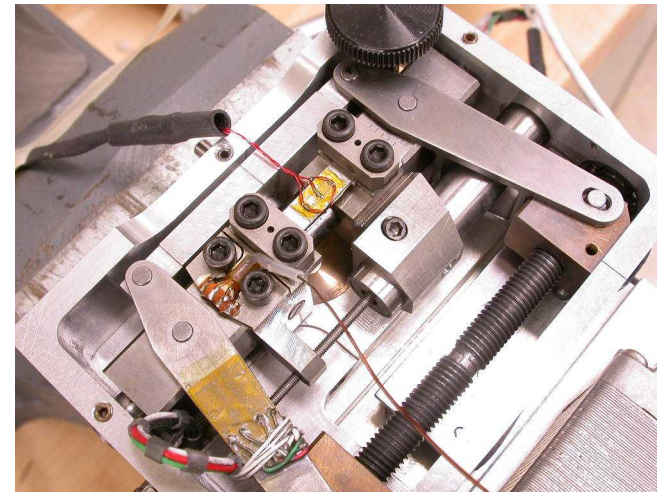
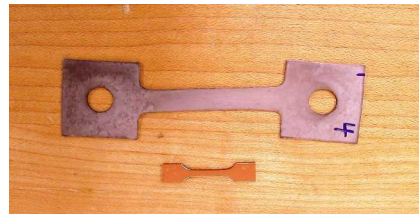
$$\sigma = \sigma_0 + \frac{c}{\max(\delta, d)^n} + \Delta \left[1 - \exp \left(-\frac{\theta}{\Delta} \varepsilon \right) \right]$$



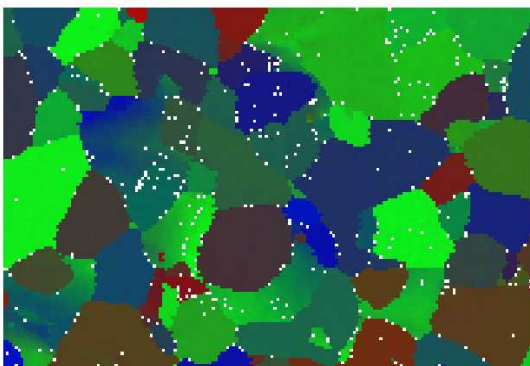
Results suggest that simply hardening grain boundaries encourages formation of subgrain structure



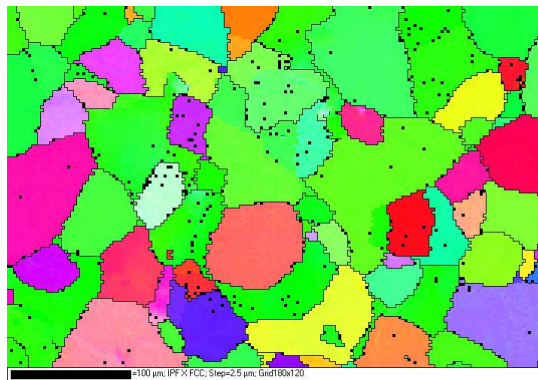
In-Situ Tensile Testing of Tantalum Samples (single crystal and polycrystalline coupons)



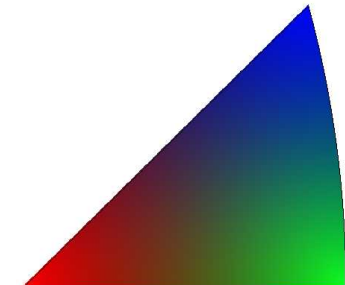
Analyzing the Ta polycrystalline sample at 0%strain



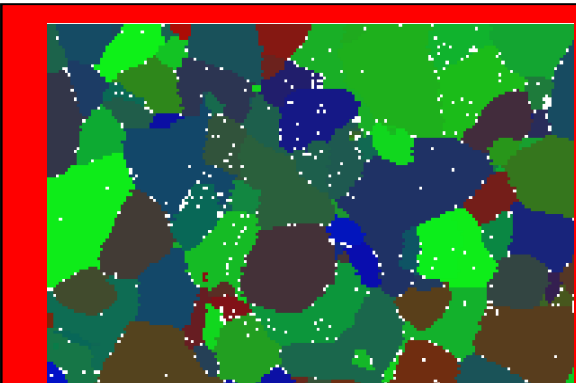
strain 0- Raw Data



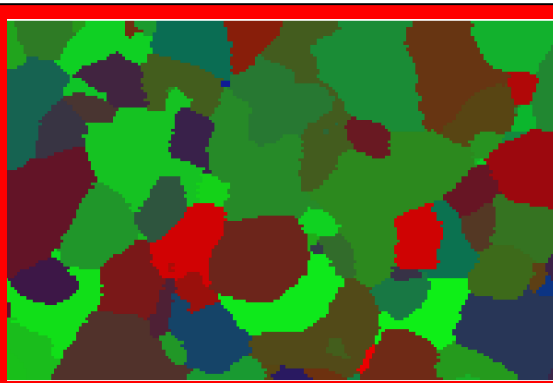
HKL map



color scheme
for EBSD maps



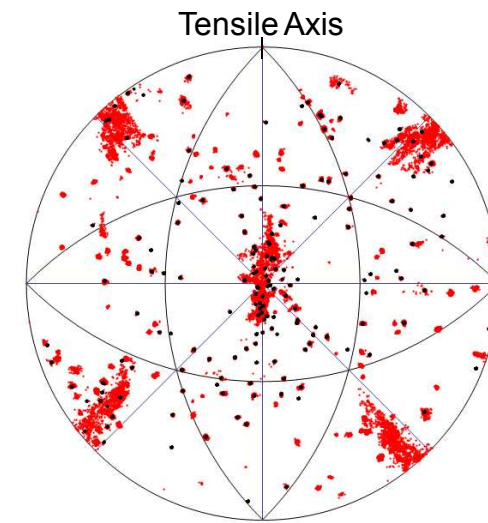
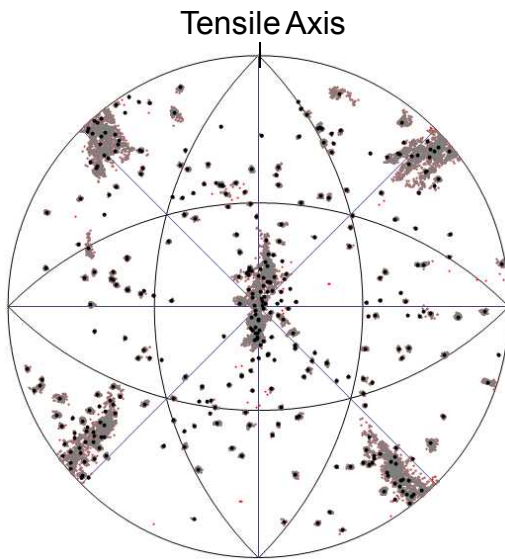
strain 0- My adaptation of quaternion
avg. method – no neighbor fill
applied



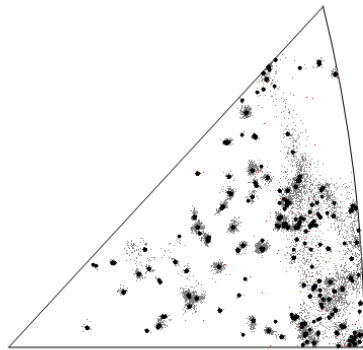
strain 0- HKL scheme for assigning a
single orientation to a grain

NOTE THE
SIGNIFICANT
DIFFERENCES
IN THE MAPS

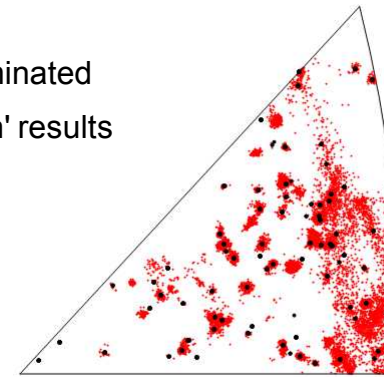
Corresponding pole figures



- raw data
- grains containing 2 pixels or less eliminated
- averaged 'single orientation per grain' results



My result – avg. orientation not determined for grain sizes two pixels or less

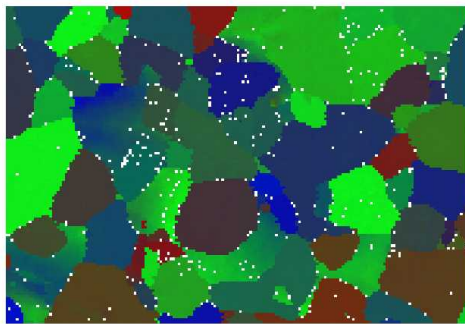


HKL algorithm for determining single orientations per grain

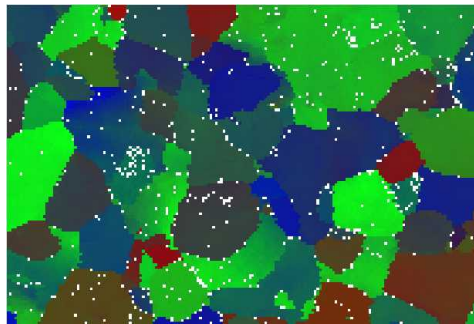
A look at microstructure evolution in deforming Ta polycrystal using EBSD

Raw Data

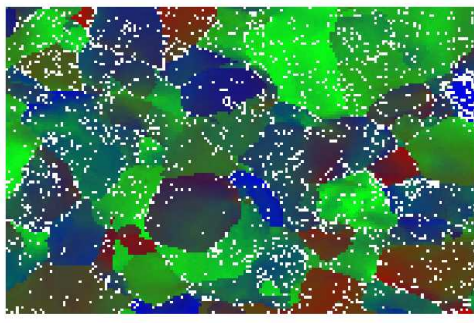
g0



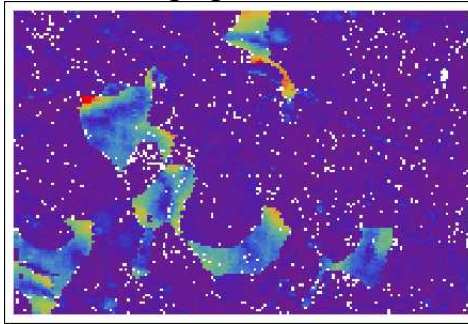
g2



g3



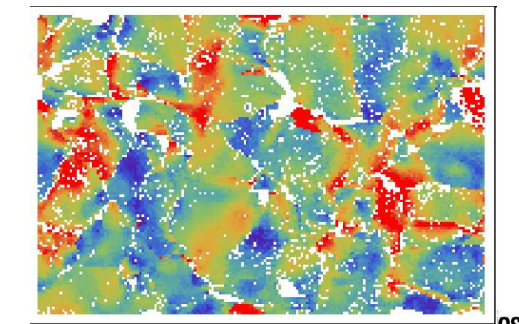
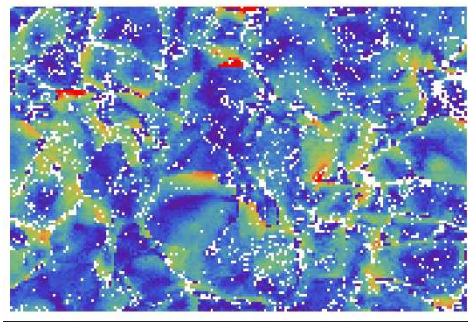
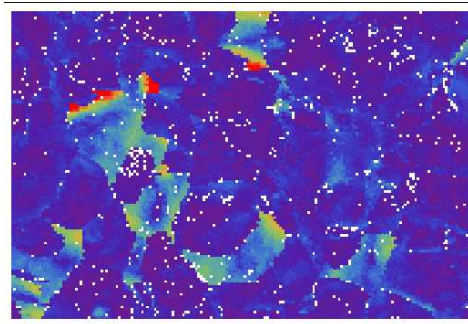
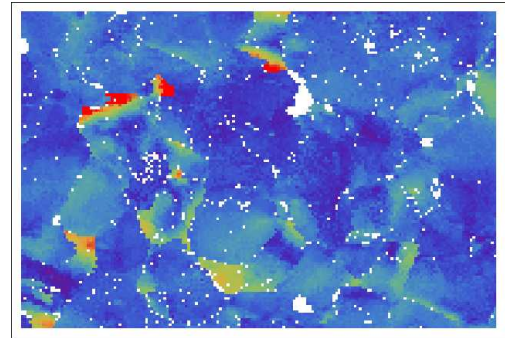
misorientation relative to current avg. grain orientation



Legend



misorientation relative to original avg. grain orientation



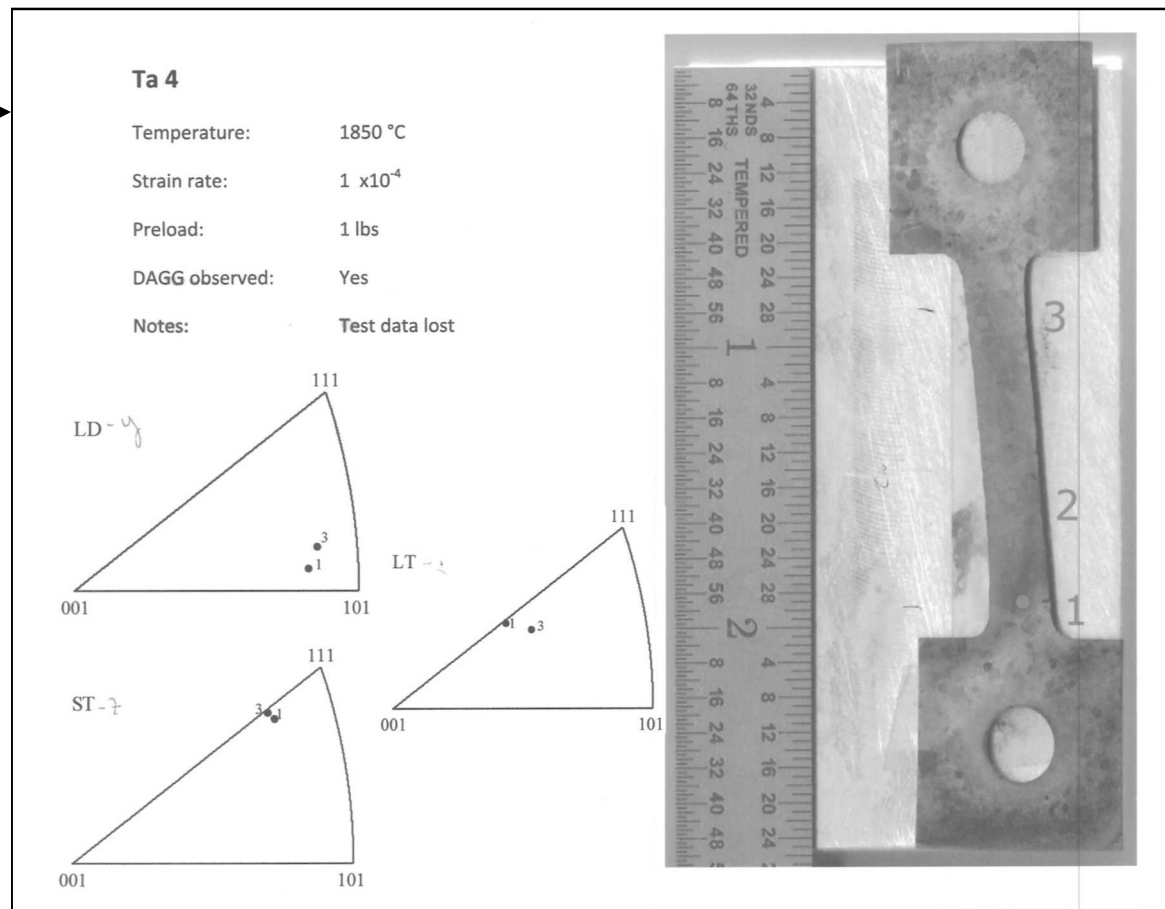
EBSD map(s) and CCI images collected near location 2 in the grip section on DAGG produced Ta Single Crystal

EBSD-Electron Backscatter Diffraction

CCI-Channel Contrast Imaging

Information sheet
provided with sample

LD (x for EBSD)
LT (Y for EBSD)
ST (Z for EBSD)

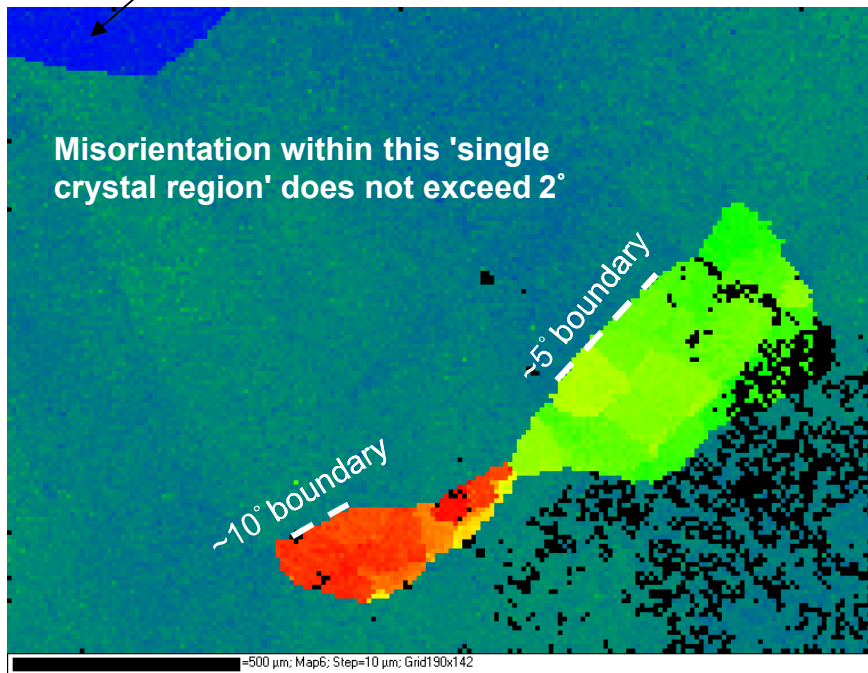


DAGG- Sample was characterized in the as-received condition

An EBSD map on Tantalum DAGG Single Crystal

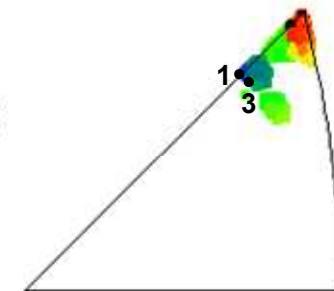
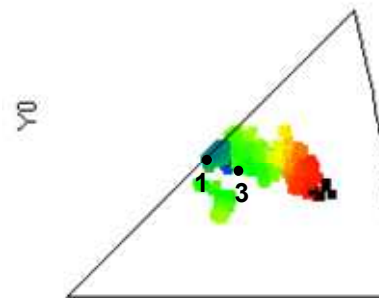
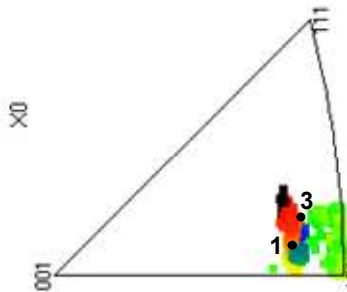
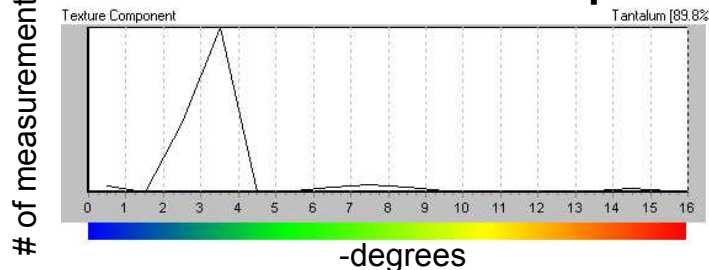
-A region selected that contained a small grain not consumed by the single crystal during the DAGG process

Reference orientation selected here



Map colorized by misorientation angle from reference. Black indicates locations that were not indexed or exceeded the max. misorientation defined for the map.

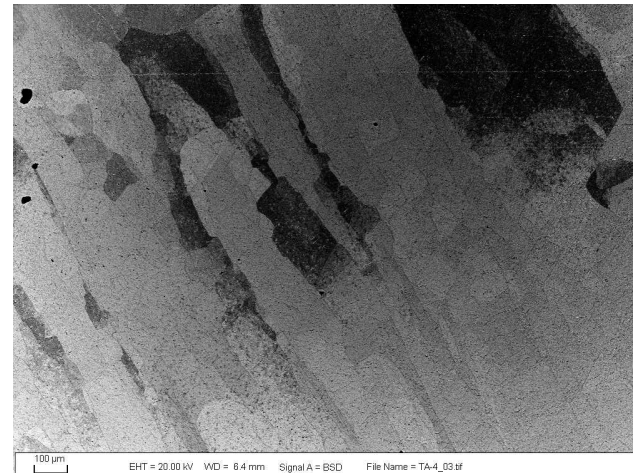
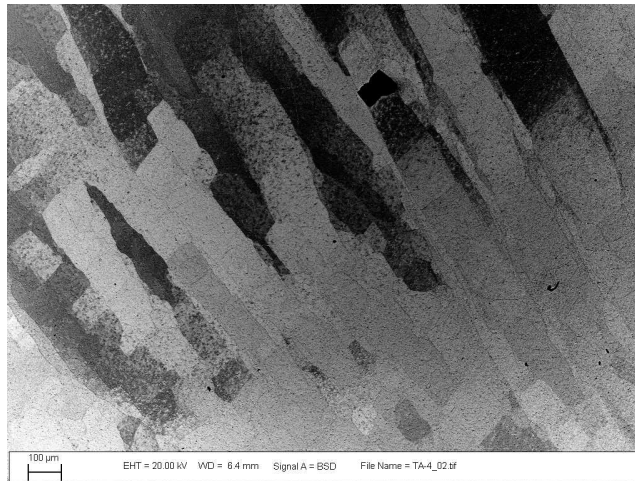
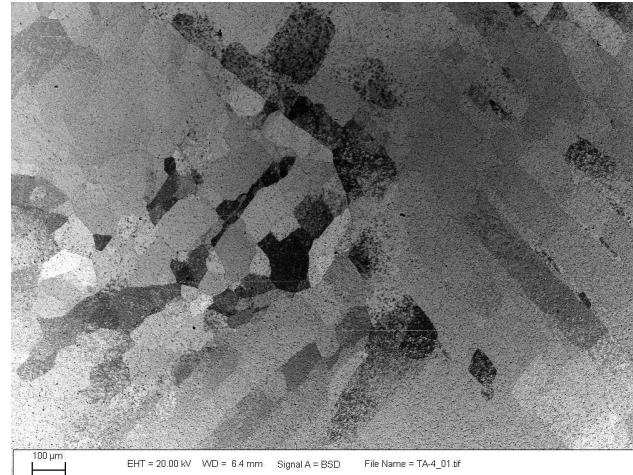
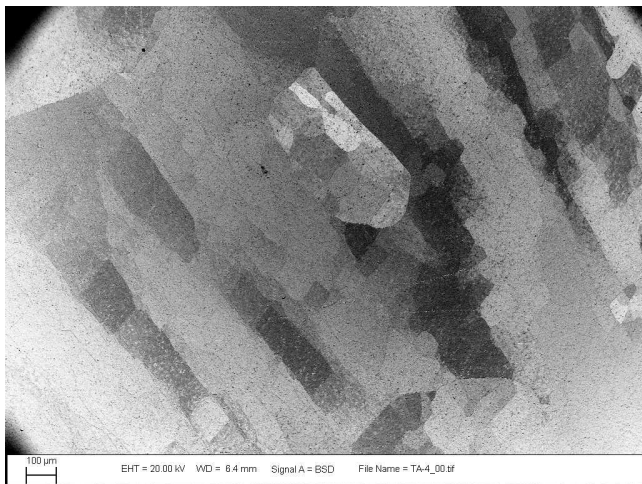
Scale used for the map



-Inverse pole figure representation of EBSD data
-UT Laue Measurements superimposed



CCI images reveal substructure in DAGG single crystal



channel contrast imaging reveals subgrain orientation changes on the order of 2°